The Timing and Structures of σ-Bond Metathesis C-H Activation Reactions

from Quasiclassical Direct Dynamics Simulations

Ryan Carlsen, Steven M. Maley, and Daniel H. Ess\*

Department of Chemistry and Biochemistry, Brigham Young University, Provo, Utah 84602.

\*E-mail: dhe@chem.byu.edu

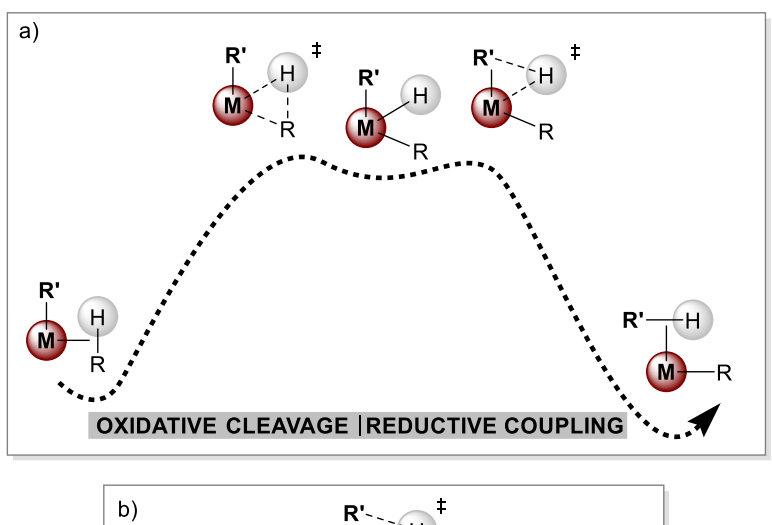
**Abstract** 

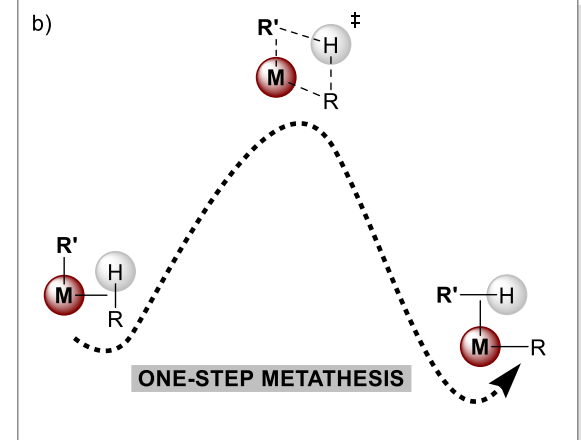
Metal-mediated  $\sigma$ -bond metathesis and  $\sigma$ -complex assisted metathesis ( $\sigma$ -CAM) reactions represent a major class of alkane C-H activation reactions. Here we present quasiclassical direct dynamics trajectories that analyze the structures and lifetimes of transition states and intermediates during Lu, Ir, and W metathesis reactions. This provides insight into the influence of atomic momentum on reaction mechanisms and whether there are non-intrinsic reaction coordinate (non-IRC) and nonstatistical pathways. For the archetype σ-bond metathesis between methane and (Cp\*)<sub>2</sub>Lu(CH<sub>3</sub>), trajectories showed this reaction to be an example of a highly concerted process with extremely rapid traversing through the transition-state region without significant Lu-H vibration. Despite our locating a (Cp\*)<sub>2</sub>Lu(CH<sub>3</sub>)(CH<sub>4</sub>) σcomplex on the potential-energy surface, this structure is always dynamically skipped, consistent with early speculation about this reaction. For the reaction of methane with (acac)<sub>2</sub>Ir(CH<sub>3</sub>), in contrast to previous DFT studies, a two-step oxidative cleavage/reductive coupling set of transition states were located. However, in contrast to the IRC motion for these reaction steps, trajectories reveal complete skipping the Ir-H intermediate, although with a few Ir-H oscillations. This reaction generally, but not always, forms a  $\sigma$ -complex, and so the term  $\sigma$ -CAM is a reasonable description. For the reaction of methane and (Cp\*)(CO)<sub>2</sub>W(BCat), dynamics trajectories show, similar to Lu metathesis, that there is no significant lifetime of a methane σ-complex prior to C-H bond cleavage and after the single metathesis transition state a highly fluxional HBCat coordination intermediate is formed.

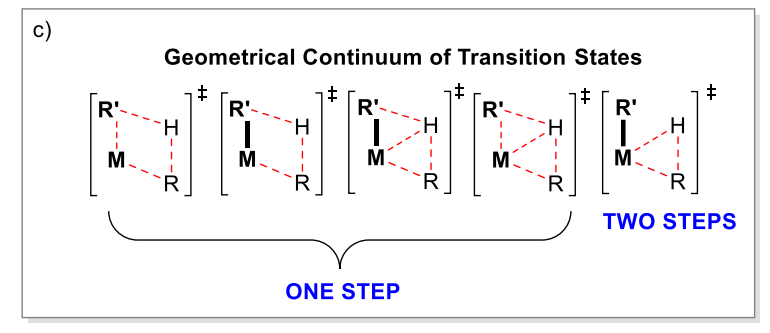
1

### Introduction

Metal-mediated C-H bond activation is a general step in the functionalization of unreactive hydrocarbons. <sup>1,2</sup> C-H activation reactions have been demonstrated across the periodic table with d-block, p-block, <sup>3</sup> and f-block<sup>4</sup> metal complexes. Applications range from methane hydroxylation to synthetic installation of functional groups in complex compounds. <sup>5,6,7,8</sup> There are two common mechanistic extremes of C-H activation reactions where the bond is broken and the hydrogen transferred to a metal ligand. The first mechanism involves a two-step sequence of oxidative cleavage and reductive coupling step with an intervening metal-hydride intermediate (Scheme 1a). <sup>9</sup> On this energy landscape, a σ-complex is generally proposed to precede oxidative cleavage and follow reductive coupling. The second common mechanism of C-H activation involves σ-bond metathesis where there is a single transition state without a metal-hydride intermediate (Scheme 1b). <sup>10</sup> This type of mechanism was originally proposed based on the reaction of (Cp\*)<sub>2</sub>Lu(CH<sub>3</sub>) with alkane isotopomers reported by Watson because no covalent metal-hydrogen interaction is possible due to the lack of oxidatively available d electrons. <sup>11,12,13,14,15</sup> Interestingly, for this Lu reaction it was assumed that no σ-complex precedes the one-step transition state for metathesis.







**Scheme 1.** a) Qualitative outline of an energy landscape and key structures for metal-mediated C-H activation involving the two-step sequence of oxidative cleavage and reductive coupling. b) Qualitative outline of an energy landscape and key structures for a one-step  $\sigma$ -bond metathesis mechanism with  $\sigma$ -complexes flaking the transition state, which is often referred to as a  $\sigma$ -CAM mechanism. c) Continuum of bonding arrangements for metal-mediated alkane C-H activation. R = alkyl group. R' = alkyl or heteroatom.

Modern examples of metal-mediated  $\sigma$ -bond metathesis almost always propose either a weak or strong  $\sigma$ -complex, and these types of reaction mechanisms are often differentiated from the Lu reaction with the term  $\sigma$ -complex assisted metathesis ( $\sigma$ -CAM). The proposal of  $\sigma$ -complexes is typically based

on isotope effects, <sup>17,18</sup> time-resolved IR, <sup>19,20</sup> potential-energy/static density functional theory (DFT) calculations, <sup>21,22,23,24</sup> and X-ray structures. <sup>25</sup> In addition to differences between the σ-bond metathesis mechanism without a σ-complex and the σ-CAM mechanism with a σ-complex, there has been demarcation of reactions based on the nature of bonding in transition-state structures. <sup>9</sup> Scheme 1c depicts the continuum of transition states identified for σ-bond metathesis and σ-CAM mechanisms. Most interesting, flanked by the extremes of oxidative cleavage with a forming metal-hydrogen bond and the traditional depiction of σ-bond metathesis with no metal-hydrogen interaction, there are several transition states with significant metal-hydrogen bonding. To date, understanding of these σ-bond metathesis and σ-CAM mechanisms has been with static DFT calculations of structures located on potential-energy surfaces and reaction pathways mapped by intrinsic reaction coordinates (IRC) calculations, which do not reveal the influence of the metal-hydrogen interaction and always lead to σ-complexes.

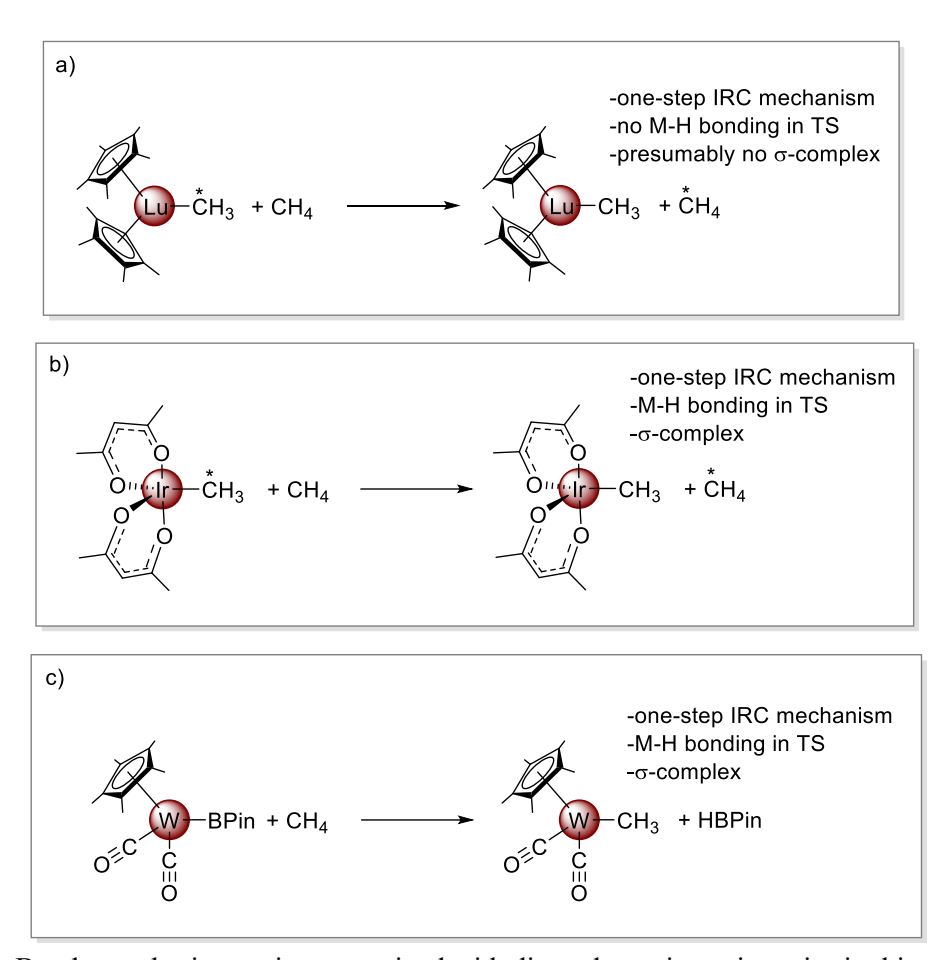
While IRCs are useful to identify connections on a potential energy surfaces through a steepest decent-type approach, as formulated by Fukui,<sup>26</sup> each point along an IRC pathway is vibrationless, rotationless, and has infinitesimal velocity. Stated another way, the potential-energy landscape and IRC only provide a possible average of structures that ascend to and descend from the transition-state structure. Our group is interested in the dynamics of metal-mediated reactions, especially for the purpose of identifying reactions with significant non-IRC or nonstatistical intermediates that generally cannot be predicted by static structures on potential-energy surfaces. In our previous direct dynamics study of the C-H activation reaction between methane and [Cp\*(PMe<sub>3</sub>)Ir(CH<sub>3</sub>)]<sup>+</sup> we found that while the DFT energy landscape showed a two-step oxidative cleavage/reductive coupling mechanism, dynamics revealed a mixture of the two-step mechanism and a new dynamical one-step mechanism that skipped the [Cp\*(PMe<sub>3</sub>)Ir(H)(CH<sub>3</sub>)<sub>2</sub>]<sup>+</sup> intermediate.<sup>27</sup> Change of the metal from Ir to Rh revealed a scenario with only a dynamical one-step mechanism.<sup>28</sup> We have also recently shown using direct dynamics simulations that although a single IRC reaction pathway was identified by DFT potential-energy calculations for the isomerization of [Tp(NO)(PMe<sub>3</sub>)W(η<sup>2</sup>-benzene)] and [Tp(NO)(PMe<sub>3</sub>)W(H)(Ph)] isomers, direct

dynamics simulations identified several new non-IRC reaction pathway connections due to the flat energy landscape.<sup>29</sup>

Because of the many different  $\sigma$ -bond metathesis and  $\sigma$ -CAM reactions, and their differences in σ-complexes and transition-state structures, we performed direct dynamics simulations to determine if they have similar or different dynamics trajectory profiles and if there are non-IRC reaction pathways or nonstatistical intermediates. We focused on Lu, Ir, and W metathesis reactions shown in Scheme 2 because of the differences in transition states and potential-energy landscapes. The reaction between methane and (Cp\*)<sub>2</sub>Lu(CH<sub>3</sub>) is an archetype metathesis transformation and originally proposed to have a single transition state, and generally assumed not to have a σ-complex (Scheme 2a). Previously disclosed potential-energy structures for this reaction show no significant Lu-H bonding in the transition state.<sup>30</sup> In contrast to the Lu metathesis reaction, the σ-CAM reaction between methane and (acac)<sub>2</sub>Ir(CH<sub>3</sub>) provides an example where there is a  $\sigma$ -complex ((acac)<sub>2</sub>Ir(CH<sub>3</sub>)(CH<sub>4</sub>)) and the previously reported one-step transition-state structure revealed significant Ir-H bonding (Scheme 2b).<sup>31</sup> The Ir-H interaction is so significant that the term oxidative hydrogen migration was been applied to describe this transformation. The  $\sigma$ -CAM reaction between methane and  $(Cp^*)(CO)_2W(BPin)$  provides an example where a boryl group, rather than methyl group, accepts the transferring hydrogen.  $^{32}$  In this case, while there is a  $\sigma$ complex before the one-step metathesis transition state the resulting HBPin is significantly different than the methane  $\sigma$ -complex.

Overall, DFT direct dynamics trajectories of these Lu, Ir, and W metathesis reactions provided key insights into the timing of bonding changes and mechanisms. For example, the σ-bond metathesis between methane and (Cp\*)<sub>2</sub>Lu(CH<sub>3</sub>) is indeed an example of a highly concerted reaction with extremely rapid traversing through the transition state region without significant Lu-H vibrations. Also, despite the location of the (Cp\*)<sub>2</sub>Lu(CH<sub>3</sub>)(CH<sub>4</sub>) σ-complex with DFT, this structure is always dynamically skipped. For the reaction of methane with (acac)<sub>2</sub>Ir(CH<sub>3</sub>), in contrast to previous DFT calculations, our DFT calculations show a two-step energy landscape, but dynamics trajectories show a dynamical one-step

mechanism, although with some Ir-H oscillations. For the metathesis reaction of methane and  $(Cp^*)(CO)_2W(BCat)$ , unexpectedly, dynamics trajectories show that there is no significant lifetime of a methane  $\sigma$ -complex prior to C-H bond cleavage and that after very fast hydrogen transfer to the BCat ligand a fluxional HBCat coordination intermediate is formed.



**Scheme 2.** σ-Bond metathesis reactions examined with direct dynamics trajectories in this work.

# **Computational Approach and Methods**

DFT structures for energy landscapes were optimized in Gaussian 09<sup>33</sup> with the M06<sup>34</sup> functional using the 6-31G\*\*[LANL2DZ for Ir, and W, SDD for Lu] basis set. The 6-31G\*\*[LANL2DZ] basis set gave nearly identical structures and relative energies of stationary points compared with Def2-type basis sets. All structures and energies were evaluated with an ultrafine integration grid. Thermochemical

corrections for enthalpies and Gibbs free energies were applied using the standard rigid rotor-harmonic oscillator approximation.

In transition state-type statistical theories, the structures located on the potential energy surface provide a representation of the average molecular trajectory for a reaction because it is assumed that there is fast equilibration between atomic kinetic energy and vibrational modes leading to complete intramolecular vibrational energy redistribution (IVR).35 Direct dynamics trajectories provide the ability to examine this assumption by directly evaluating time-dependent geometry changes, which can identify non-IRC and nonstatistical reaction pathways.<sup>36</sup> Direct dynamics trajectories are advantageous because forces needed for propagation of trajectories are evaluated at every time step with DFT. Trajectory calculations in this work were carried out in Gaussian 09<sup>33</sup> with M06/6-31G\*\*[LANL2DZ] and the ultrafine integration grid. From each  $\sigma$ -bond metathesis and  $\sigma$ -CAM reaction transition state, initialization of quasiclassical trajectories was done using local mode and thermal sampling at 298 K, which includes zero-point energy (ZPE). Trajectories were propagated in mass-weighted Cartesian velocities with an approximate average step of 0.6 femtoseconds (fs), which we previously showed for organometallic reactions is a short enough time step to give results identical to time steps as small as 0.25 fs. <sup>27</sup> Forward trajectories were launched so that the transition-state vibrational mode was followed in the direction for increasing the length of the breaking methane C-H bond. Reverse trajectories followed the direction of decreasing this C-H bond length. Both the gradient and Hessian were updated at each time step.

### **Results and Discussion**

Previous DFT Calculations and Static Potential-Energy Surfaces. In 2003, Cramer used B3LYP and mPWPW91 density functionals to determine structures and energies for σ-bond metathesis reactions between methane and Sc, Y, and Lu-based metallocenes (Cp\*<sub>2</sub>M(CH<sub>3</sub>)).<sup>30</sup> Cramer's DFT data suggests that formation of a tuck-in complex is 5-10 kcal/mol higher than the bimolecular σ-bond metathesis pathway (Schemes 1b and 3a). The B3LYP DFT method predicted a σ-bond metathesis barrier

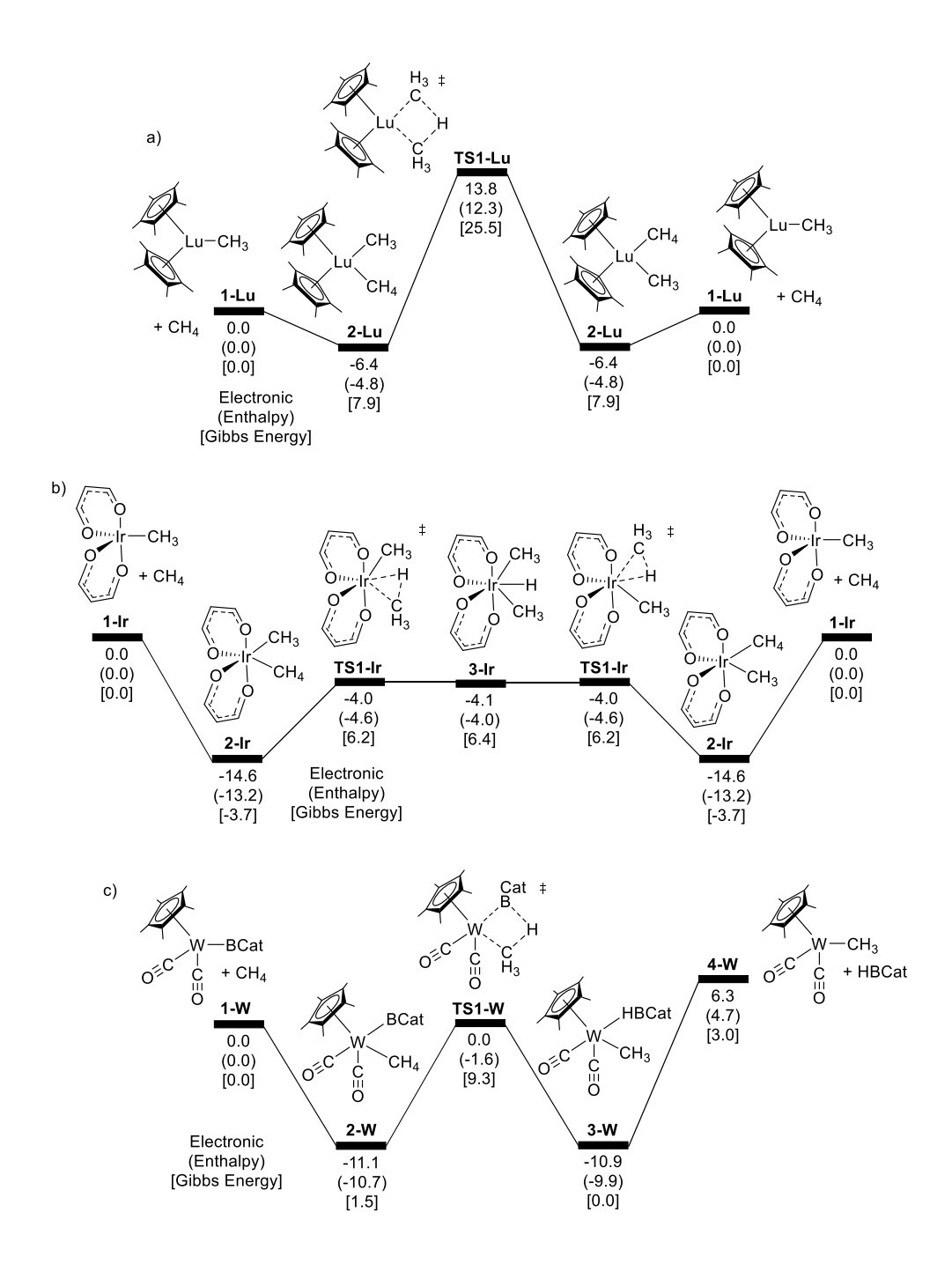
nearly double the experimental enthalpy value of 11.6 kcal/mol for  $Cp*_2Lu(CH_3)$ , although the data for this experimental barrier estimate to our knowledge was never fully published. Cramer suggested that tunneling corrections might account for the difference between the B3LYP calculated and experimental barriers. Cramer evaluated a one-dimensional tunneling estimate, which lowered the barrier by  $\sim$ 7 kcal/mol. Subsequent to the Cramer study, Eisenstein and Maron used B3PW91 to examine the  $\sigma$ -bond metathesis between methane and  $Cp*_2Lu(CH_3)$  and reported and activation enthalpy of 19.8 kcal/mol.<sup>37</sup>

Cramer also examined the  $\sigma$ -bond complex prior to and after the one-step transition state. The use of model chloride ligands rather than Cp\* groups resulted in the location of relatively stabilized methane  $\sigma$ -complexes. However, with Cp\* ligands, as expected due to the larger donor capacity of the ligand, Cramer described the located  $\sigma$ -complexes as very loose, very weak van der Waals type complexes.

Our M06 energy landscape is different than the previous B3LYP and B3PW91 surfaces. Scheme 3a shows the M06 energy landscape for reaction between  $Cp*_2Lu(CH_3)$  and methane. With M06 the methane  $\sigma$ -bond complex  $[Cp*_2Lu(CH_3)(CH_4)]$  **2-Lu** is exothermic relative to separated  $Cp*_2Lu(CH_3)$  **1-Lu** and methane. Previous DFT values for **2-Lu** showed this  $\sigma$ -complex to be higher in enthalpy than separated structures. This is likely because previous DFT functionals did not significantly account for dispersion interactions. With M06, the  $\Delta H^{\ddagger}$  value for **TS1-Lu** relative to separated **1-Lu** and methane is 12.3 kcal/mol, which is close to the experimental value of 11.6 kcal/mol. However, the  $\Delta H^{\ddagger}$  value for **TS1-Lu** relative to **2-Lu** is 17.1 kcal/mol, which is potentially too large compared to experiment. These M06 values change by less than 2 kcal/mol with very large basis sets, such as def2-TZVPP or with continuum cyclohexane solvent. We have also compared our M06 results to DLPNO-CCSD(T) values (see the Supporting Information (SI)). Despite the enthalpy of **2-Lu** being lower than **1-Lu**, the Gibbs energy surface suggests that this  $\sigma$ -complex is higher in energy.

As demonstrated by Cramer, there is the possibility of tunneling impacting the rate of this Lu  $\sigma$ -bond metathesis reaction. While we could not find an experimental  $k_{\rm H}/k_{\rm D}$  kinetic isotope effect (KIE) for the reaction between methane and Cp\*<sub>2</sub>Lu(CH<sub>3</sub>), Watson reported a  $k_{\rm H}/k_{\rm D}$  estimate of 5.5 for the reaction

between Cp\*<sub>2</sub>Lu(CH<sub>3</sub>) and benzene-*d*<sub>6</sub>. <sup>11,12</sup> Using zero-point energies from the benzene and benzene-*d*<sub>6</sub> versions of **TS1-Lu**, our calculated KIE value is 4.1, which is close to the experimental value, which suggests that our quasiclassical dynamics trajectories presented later that do not include tunneling effects likely portray the major kinetic pathway.



**Scheme 3.** M06/6-31G\*\*[LANL2DZ for Lu, Ir, and W] energy landscapes for the reactions of methane with a) (Cp\*)<sub>2</sub>Lu(CH<sub>3</sub>), b) (acac)<sub>2</sub>Ir(CH<sub>3</sub>) (methyl groups were omitted from the acac ligand structure), and c) Cp\*(CO)<sub>2</sub>W(BCat). Energies in kcal/mol.

The  $\sigma$ -bond metathesis reaction between [(acac)<sub>2</sub>Ir(CH<sub>3</sub>)(pyridine)] and a variety of alkanes was demonstrated by Periana.<sup>38</sup> Based on experimental studies, it was proposed that the reactive species (acac)<sub>2</sub>Ir(CH<sub>3</sub>) (1-Ir) induces a C-H bond metathesis process through either the one-step  $\sigma$ -bond metathesis mechanism or the two-step oxidative cleavage/reductive coupling sequence. B3LYP DFT calculations were used to locate a one-step  $\sigma$ -CAM transition state that is symmetric for the C-H bond breaking and C-H bond forming and with a short and strong Ir-H interaction. Also, this single transition state showed a direct potential-energy connection to a  $\sigma$ -complex.

In contrast to the Lu metathesis reaction, with M06, the [(acac)<sub>2</sub>Ir(CH<sub>3</sub>)(CH<sub>4</sub>)] σ-complex **2-Ir** is both exothermic and exergonic relative to **1-Ir** and methane. With expectations based on the previous B3LYP calculations, we were surprised when our M06 calculations located the (acac)<sub>2</sub>Ir(H)(CH<sub>3</sub>)<sub>2</sub> structure **3-Ir** and an unsymmetrical oxidative cleavage and reductive coupling transition state **TS1-Ir**. This means that caution should be exercised when defining a one-step versus two-step potential-energy mechanism when using just a single density functional method. Additionally, our own use of B3LYP showed a two-step mechanism, not a one-step mechanism. More importantly, **3-Ir** is only 0.1 kcal/mol above **TS1-Ir** on the electronic energy surface, this intermediate is 0.4 and 0.2 kcal/mol higher than **TS1-Ir** on the enthalpy and Gibbs surfaces, which suggests a very flat energy surface in the region of the structure and the lifetime of this intermediate will be significantly influenced by dynamic effects.

One of the most prominent examples of a metal-boryl complex inducing C-H activation through a  $\sigma$ -CAM mechanism involves the reaction of photo-generated (Cp\*)(CO)<sub>2</sub>W(BR<sub>2</sub>) with alkanes reported by Hartwig.<sup>39</sup> B3LYP DFT transition states by Hall revealed a one-step  $\sigma$ -CAM mechanism that avoids formal W oxidation.<sup>40</sup> DFT calculations also provided evidence for the  $\sigma$ -complex [(Cp\*)(CO)<sub>2</sub>W(B(OR)<sub>2</sub>)(RH)] before the metathesis transition state and the borane  $\sigma$ -complex

 $[(Cp^*)(CO)_2W(R)(HB(OR)_2)]$  after the transition state. The  $\sigma$ -CAM transition state was described as a three-center four-electron process with a small amount of metal-hydride bonding. After the borane  $\sigma$ -complex  $[(Cp^*)(CO)_2W(R)(HB(OR)_2)]$  is formed it rearranges to then undergo a second  $\sigma$ -CAM transition state to generate the alkylborane product.

Our M06 calculated potential-energy landscape for the reaction of methane and with  $(Cp^*)(CO)_2W(CH_3)$  is shown in Scheme 3a. The enthalpy barrier from **2-W** to **TS1-W** is 11.7 kcal/mol, which is very similar to the B3LYP barrier reported by Hall. The only significant difference between the previous B3LYP energy surface and the M06 surface is that the  $(Cp^*)(CO)_2W(CH_3)(HBCat)$  complex is close to the energy of the methane  $\sigma$ -complex while on the B3LYP surface this structure is several kcal/mol endothermic.

Dynamics Trajectories. Prior to our work, only a single study examined dynamic motion of a σ-bond metathesis reaction with Lu. Maron used Car-Parrinello type molecular dynamics, which is significantly different that the quasiclassical trajectories used in this work, to examine the model reaction between Cl<sub>2</sub>Lu(H) and Cl<sub>2</sub>Lu(CH<sub>3</sub>) with H<sub>2</sub>.<sup>41</sup> In Maron's work the focus was on comparing static potential-energy structures and their thermodynamic and kinetic values with those obtained from Car-Parrinello dynamics. This Car-Parrinello study did suggest that the energy surface surrounding the transition state is relatively flat, although it was unclear if this was a result of using model chloride ligands rather than Cp\* ligands.

52 quasiclassical trajectories for the reaction between methane and Cp\*<sub>2</sub>Lu(CH<sub>3</sub>) were initiated at **TS1-Lu** and propagated in forward and reverse directions. Only one out of 52 trajectories showed recrossing and began forward progression of the hydrogen to the methyl ligand and then reversed course and returned to forming the original methane C-H bond. A representative non-recrossing trajectory is shown in Figure 1. The first snapshot (Step 1) begins at the transition state. Within 100 steps, with an average time step of ~0.7 fs, the hydrogen from methane is fully transferred to the methyl ligand. From Step 100 to 250 the newly formed methane directly dissociates from the Lu metal center without

significant loitering at a σ-complex. To inspect the timing of hydrogen transfer and methane dissociation, Figure 2 plots the Lu-H distance versus trajectory step for all forward trajectories from the transition state. In all cases, between 35-50 fs the hydrogen is completely transferred to the methyl ligand and methane dissociation begins. Between 50-175 fs the methane is within van der Waals distance, but there is constant, nearly uninhibited motion of methane away from the Lu metal center. By 150 fs every trajectory shows complete methane dissociation. This suggests that this reaction should be regarded as an extremely fast concerted  $\sigma$ -bond metathesis process and there is no significant lifetime of a  $\sigma$ -complex, despite its location on the potential-energy surface. Further evidence for the description of a highly concerted hydrogen transfer comes from the analysis of Lu-H vibrational oscillations during transfer. Between the transition state and when the Lu-H distance exceeded 2.25 Å there were only on average 1.6 bond oscillations, revealing no significant lifetime of an oxidized Lu-H intermediate. As a comparison, we also examined 20 trajectories for the reaction between methane and Cp\*2Sc(CH3). These trajectories showed nearly identical behavior to the Lu trajectories with extremely fast traversing of the transition-state zone and uninhibited extrusion of methane from the Sc metal center (see SI for plots). Importantly, these are gas phase transition states and trajectories and show the intrinsic skipping of the  $\sigma$ -complex. State another way, the Lu and Sc metal centers do not provide enough attraction to keep the methane tightly coordinated after the motion of the transition state. However, it is possible that trajectories with explicit cyclohexane solvent would show a cage effect where methane would return to the metal center by rebounding from collision with a solvent cyclohexane, but it is not clear if this would lead to a long-lived  $\sigma$ -complex intermediate.

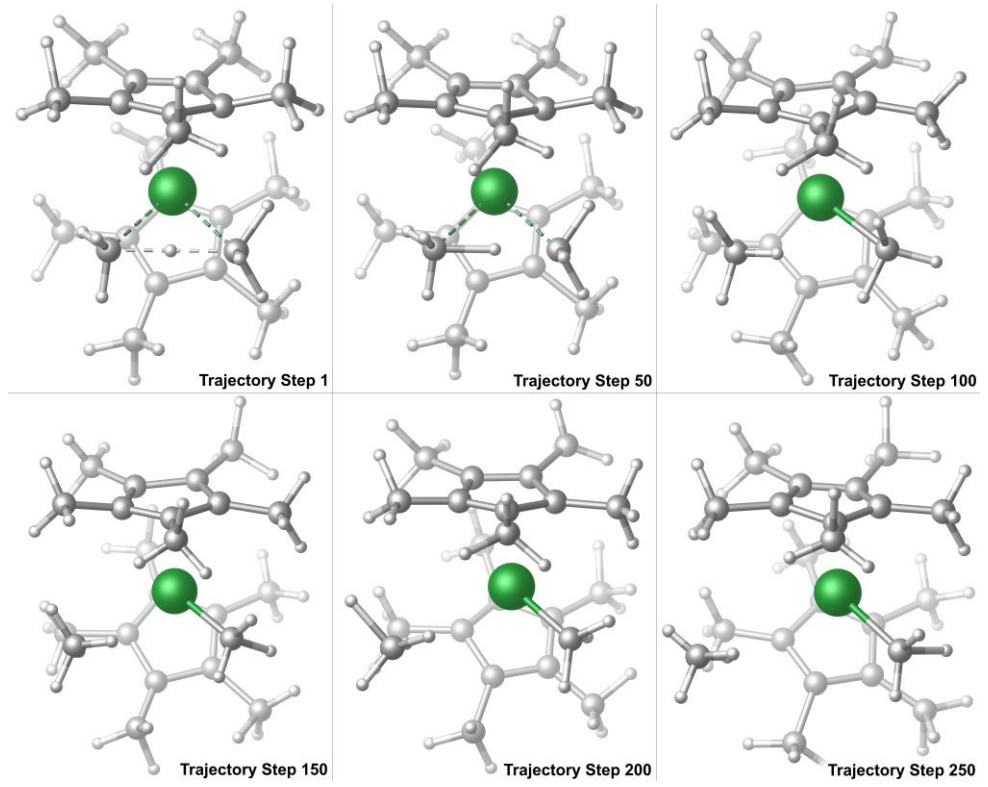


**Figure 1.** Snapshots of a representative trajectory initiated at the  $\sigma$ -bond metathesis transition state **TS1-Lu**. Each trajectory time step is on average 0.7 fs.

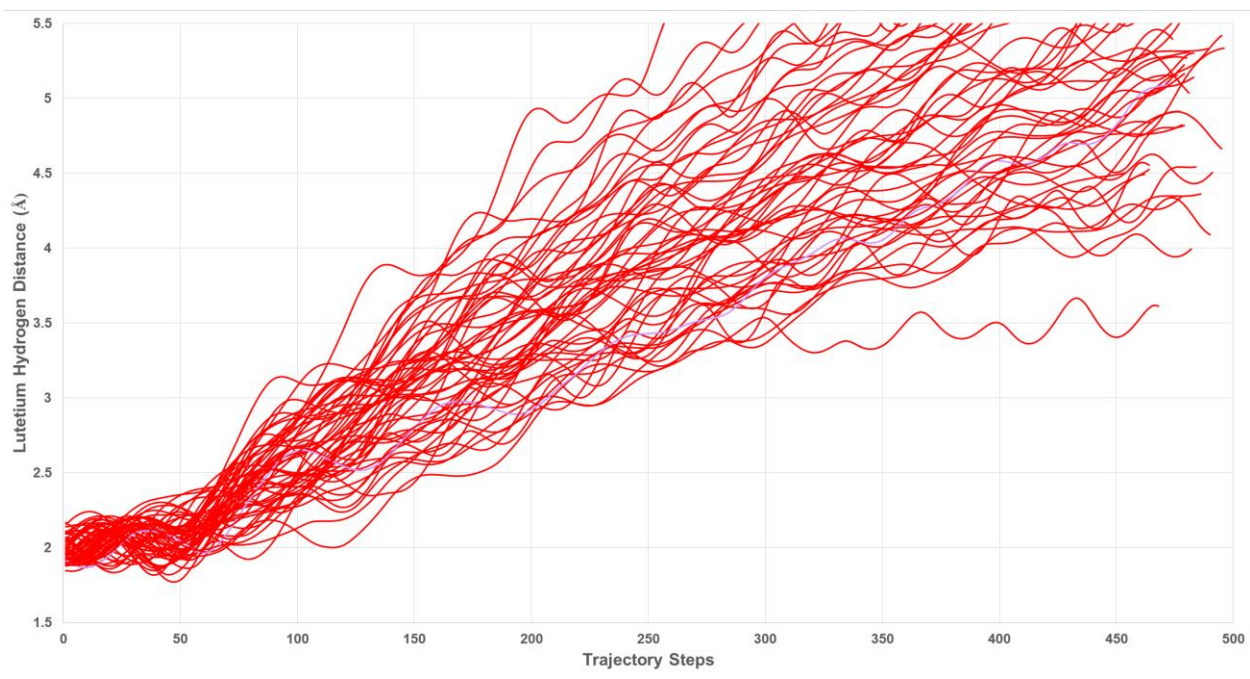


**Figure 2.** Lu-H distance for each trajectory in the forward direction starting at the transition state, **TS1-Lu**. Red trajectories progress to complete dissociation in the forward direction while lavender trajectories recross. Each trajectory time step is on average 0.7 fs.

The skipping of the σ-complex **2-Lu** is somewhat similar to what we previously found for the reaction between [Cp\*(PMe<sub>3</sub>)Ir(CH<sub>3</sub>)]<sup>+</sup> with methane, but very different from what we found for the methane reductive elimination from [(PONOP)Rh(H)(CH<sub>3</sub>)]<sup>+</sup>. Importantly, direct methane dissociation occurs in both the forward and reverse reaction directions. This indicates that there is no long-lived σ-complex and that thermodynamics and kinetics should be based on a comparison between dissociated methane and Cp\*<sub>2</sub>Lu(CH<sub>3</sub>) and that the complex [Cp\*<sub>2</sub>Lu(CH<sub>3</sub>)(CH<sub>4</sub>)] likely does not contribute to the experimental activation enthalpy measurement. From this perspective, the M06 enthalpy barrier of 12.3 kcal/mol is close to the experimental value. Temperature corrections do not significantly change the barrier height estimate. However, this DFT values is likely fortuitously close to experiment since DLPNO-CCSD(T)<sup>42</sup> energies for **1-Lu** to **TS1-Lu** show several kcal/mol higher barrier (see SI). While tunneling is likely to occur in this reaction, as demonstrated from Cramer's estimate, this type of reaction mechanism is unlikely to dominate the reaction mechanism. However, from one perspective, a tunneling type mechanism in the vicinity of the transition-state zone likely enhances the description of this reaction be a concerted, one-step, extremely fast σ-metathesis pathway. The lack of recrossing with a relatively flat transition-state zone also suggests a highly concerted mechanism.

55 quasiclassical trajectories for the reaction between methane and (acac)<sub>2</sub>Ir(CH<sub>3</sub>) were initiated at **TS1-Ir** and propagated in forward and reverse directions. Figure 3 plots the breaking methane C-H bond distance versus trajectory steps, which are on average 0.7 fs. In contrast to the Lu σ-bond metathesis reaction that showed very little recrossing, Figure 3 shows that nearly 1/3 of Ir trajectories (lavender color) recross. All the non-recrossing trajectories (green and red) show relatively rapid increase from ~1.5 Å to >2.5 Å between the transitions state and ~140 fs (200 time steps). This indicates that while the (acac)<sub>2</sub>Ir(H)(CH<sub>3</sub>)<sub>2</sub> **3-Ir** structure that was located on the potential-energy surface this intermediate is skipped. With all trajectories showing the Ir-H intermediate skipped, this contrasts with the reaction [Cp\*(PMe<sub>3</sub>)Ir(CH<sub>3</sub>)]<sup>+</sup> with methane where only about 10% of the trajectories skip the oxidized

intermediate. While the Ir-H intermediate is skipped, it is not as concerted as the Lu reaction. During these skipping trajectories, from **TS1-Ir** to the formation of the new C-H bond there are on average approximately five Ir-H oscillations, although this should not be considered an intermediate since no significant IVR occurs.



**Figure 3.** Iridium hydrogen distance for the trajectory ensemble. Red trajectories proceed to separated (acac)<sub>2</sub>Ir(CH<sub>3</sub>) and methane, green trajectories proceed to the sigma-complex intermediate, and lavender trajectories recross. Each trajectory step is on average 0.7 fs.

From 200 time steps ( $\sim$ 140 fs) to 400 time steps ( $\sim$ 280 fs), the breaking methane C-H distance continues to increase and two different types of trajectories become apparent. The majority green trajectories result in formation of the  $\sigma$ -complex with a C-H distance fluctuating between  $\sim$ 3-5 Å. This fluctuation occurs due to the tumbling motion of methane and scrambling of the C-H bond that is closest to the Ir metal center. The minor red trajectories show a C-H distance indicative of complete methane dissociation, which while may not necessarily be anticipated based on the potential-energy surface shown in Scheme 3b, the energy of **TS1-Ir** is close to the overall energy of separated species. Overall, with most trajectories showing a  $\sigma$ -complex and the Ir-H intermediate always being skipped the  $\sigma$ -CAM description is appropriate. Figure 4 shows snapshots of a representative trajectory that skips the Ir-H intermediate and

forms the  $\sigma$ -complex **2-Ir**. It is important to contrast this trajectory with one of the trajectories that skips the Ir-H intermediate and ejects methane, which is shown in Figure 5. In this latter trajectory, after methane completely dissociates from the Ir metal sphere, there is isomerization of the acac ligands from an initial relative *cis* configuration to a *trans* configuration. This *cis*-to-*trans* isomerization is very rapid and requires approximately 75 fs. Because of the very fast timing between methane dissociation and isomerization, it is very likely that complete methane dissociation from the Ir center is correlated and coupled with isomerization motion. This is reasonable since the *cis*-to-*trans* transition state is only ~5 kcal/mol higher in energy than the energy of the *cis*-(acac)<sub>2</sub>Ir(CH<sub>3</sub>) structure. Also, this is the first report of ligand motion being dynamically coupled with inner-sphere metal-mediated covalent bonding changes.

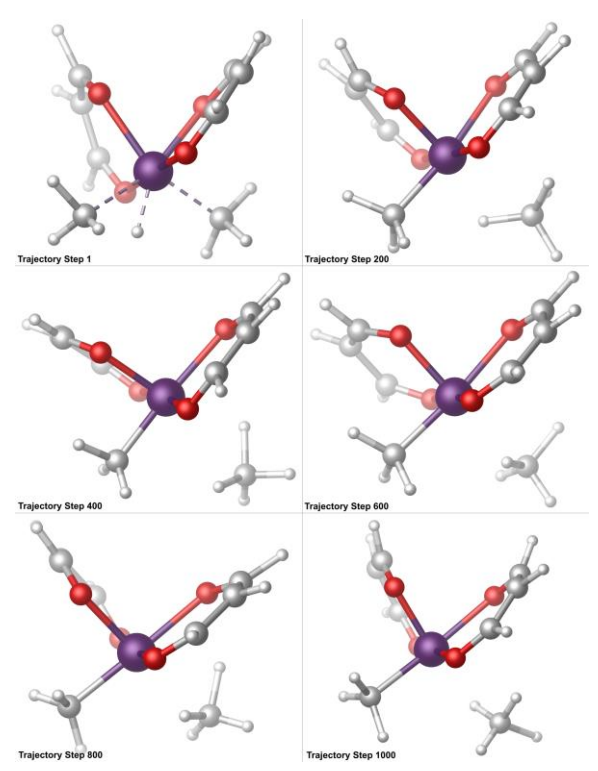


**Figure 4.** Snapshots of a representative trajectory initiated at **TS1-Ir** and stopping at the  $\sigma$ -complex.

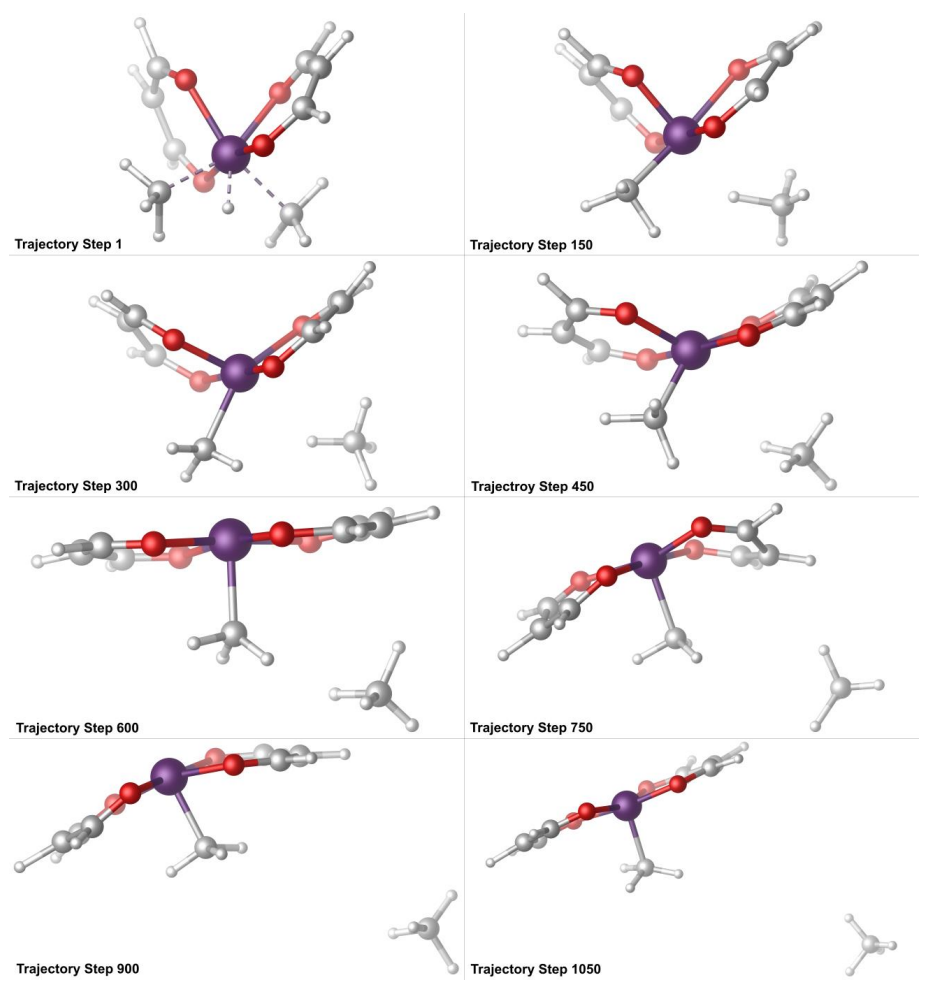


**Figure 5.** Snapshot of a trajectory initiated at **TS1-Ir** leading methane dissociation and *cis*-to-*trans* ligand isomerization. Each trajectory step is on average 0.7 fs.

As a comparison to the Lu and Ir metathesis reactions, we also propagated 34 trajectories for the reaction between methane and  $(Cp^*)(CO)_2W(BCat)$ . Figure 6 plots the W-C distance for trajectories in the reverse direction towards **2-W** starting from **TS1-W**. In this case methane dissociation occurred in about 25% of the trajectories, despite **2-W** being 10.7 kcal/mol more stable than separated structures. This suggests that the term  $\sigma$ -CAM does not completely apply to this reaction, at least for the C-H activation step, and some of the trajectories are more akin to the Lu metathesis process than the Ir metathesis reaction.

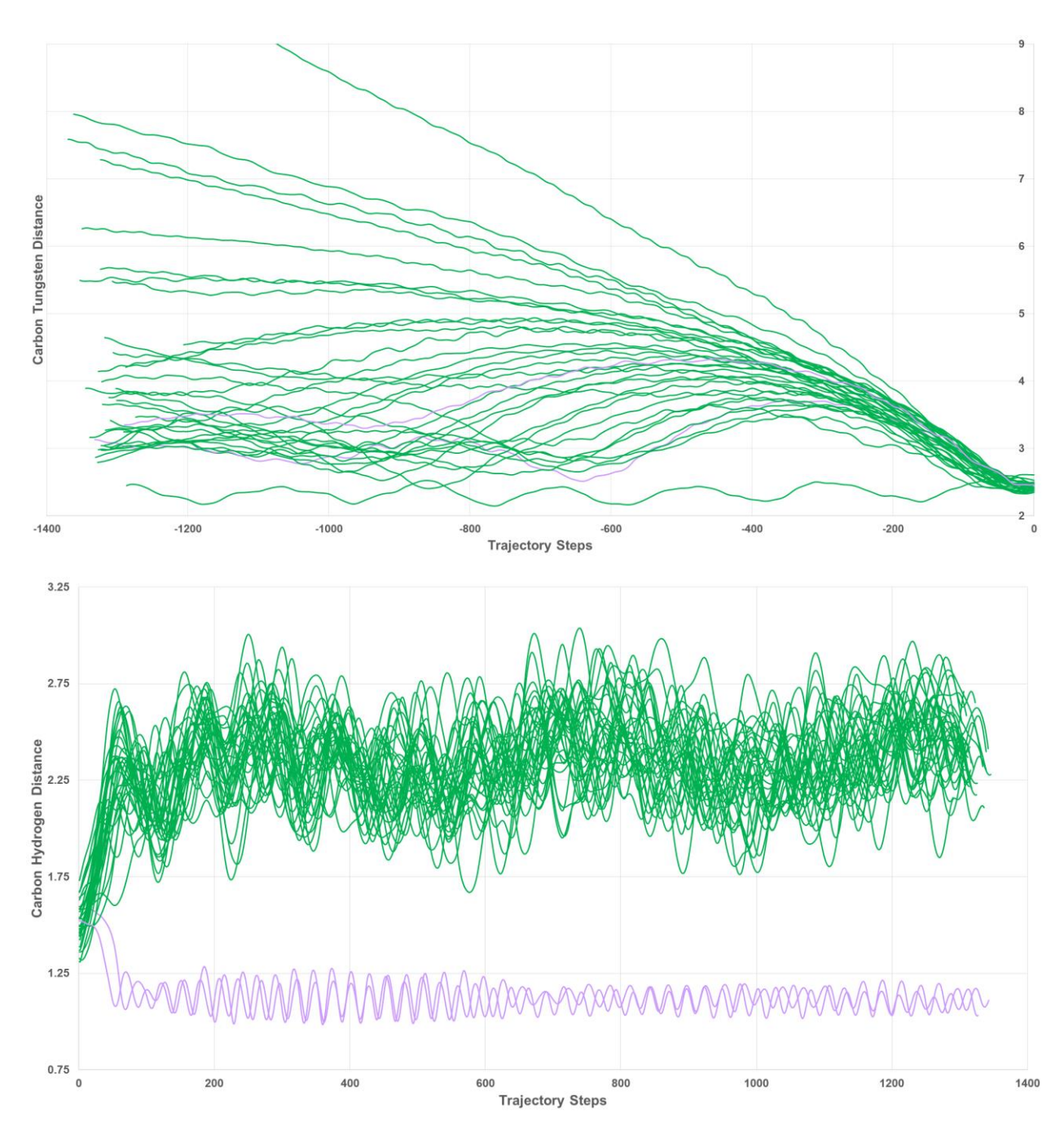


**Figure 6.** Top: W-C distance for each trajectory in the reverse direction starting at the transition state, **TS1-W**. Green trajectories progress to intermediate in the forward direction while lavender trajectories recross. Each trajectory time step is on average 0.7 fs. Distances are in Angstroms. Bottom: C-H distance for each trajectory in the forward direction starting at the transition state, **TS1-W**. Green trajectories progress to intermediate in the forward direction while lavender trajectories recross. Each trajectory time step is on average 0.7 fs. Distances are in Angstroms.

In the forward direction from **TS1-W** towards **3-W** there is only a small number of trajectories that showed recrossing. Most trajectories showed very fast completion of C-H bond breaking and B-H bond formation and resulted in the formation of the borane σ-complex **3-W**. A representative trajectory is displayed in Figure 7. At the transition state the breaking C-H bond is highly stretched and there is very little movement of the hydrogen to complete transfer to the BCat ligand, which in this trajectory is complete by step 150. After hydrogen transfer to the BCat ligand, the remainder of all trajectory time shows B-H bond oscillations coordinated to the W metal center. Due to charge-transfer bonding with the W metal center, these B-H oscillations are centered at a length of 1.34 Å, which is longer than for free HBCat where trajectories show oscillations centered at 1.2 Å.

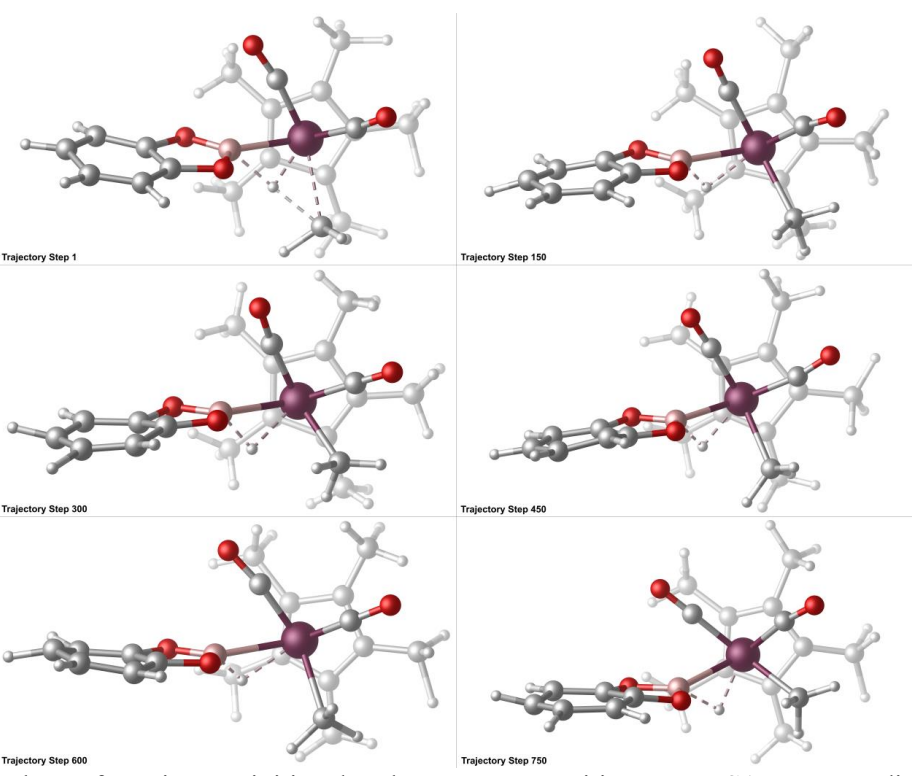


**Figure 7**. Snapshots of a trajectory initiated at the  $\sigma$ -CAM transition state **TS1-W** proceeding to a sigma complex intermediate. Each trajectory step is on average 0.7 fs.

## **Conclusions**

Quasiclassical dynamics trajectories provided analysis of the structures and lifetimes of transition states and intermediates for Lu, Ir, and W metathesis reactions. For the metathesis between methane and  $(Cp^*)_2Lu(CH_3)$ , trajectories showed this reaction to be an example of a highly concerted process with extremely rapid traversing through the transition-state region and essentially no Lu-H vibration. Despite a  $(Cp^*)_2Lu(CH_3)(CH_4)$   $\sigma$ -complex on the potential-energy surface, this structure is always dynamically skipped. However, these are gas phase trajectories that show the intrinsic skipping of the  $\sigma$ -complex and it is possible that trajectories with explicit cyclohexane solvent would show a cage effect where methane would return to the metal center by rebounding from collision with a solvent cyclohexane. In this type of scenario, it is not clear if this would lead to a long-lived  $\sigma$ -complex intermediate. For the reaction of methane with  $(acac)_2Ir(CH_3)$ , in contrast to previous DFT calculations, a two-step reaction pathway was identified. However, trajectories revealed complete skipping the Ir-H intermediate in a dynamical one-step mechanism. This reaction generally, but not always, forms a  $\sigma$ -complex. For the reaction of methane and  $(Cp^*)(CO)_2W(BCat)$ , dynamics trajectories show, similar to Lu metathesis that in about 25% pf the trajectories there is no significant lifetime of a methane  $\sigma$ -complex prior to C-H bond cleavage and after the single metathesis transition state a highly fluxional HBCat coordination intermediate is formed.

# Acknowledgments

We thank Brigham Young University and the Office of Research Computing, especially the Fulton Supercomputing Lab. R. C. thanks BYU Graduate Division for a HIDRA fellowship. D.H.E. acknowledges the United States National Science Foundation Chemical Structure, Dynamics, and Mechanisms B (CSDM-B) Program for support under award CHE 1952420.

#### **Declarations**

The authors declare no competing financial interests.

### References

- 1. Bergman, R. G. C-H Activation. *Nature* **2007**, *446*, 391–393.
- 2. Hartwig, J. F. Evolution of C–H Bond Functionalization from Methane to Methodology. *J. Am. Chem. Soc.* **2016**, *138*, 2–24.
- 3. Hashiguchi, B. G.; Konnick, M. M.; Bischof, S. M.; Gustafson, S. J.; Devarajan, D.; Gunsalus, N.; Ess,
- D. H.; Periana, R. A. Main-Group Compounds Selectively Oxidize Mixtures of Methane, Ethane, and Propane to Alcohol Esters. *Science* **2014**, *343*, 1232–1237.
- 4. Yamanaka, I.; Soma, M.; Oisuka, K. Oxidation of methane to methanol with oxygen catalysed by europium trichloride at room temperature. *J. Chem. Soc.*, *Chem. Commun.* **1995**, 2235–2236.
- 5. Periana, R. A.; Taube, D. J.; Gamble, S.; Taube, H.; Satoh, T.; Fujii, H. Platinum catalysts for the high-yield oxidation of methane to a methanol derivative. *Science* **1998**, *280*, 560–564.
- 6. Gunsalus, N. J.; Koppaka, A.; Park, S. H.; Bischof, S. M.; Hashiguchi, B. G.; Periana, R. A. Homogeneous Functionalization of Methane. *Chem. Rev.* **2017**, *117*, 8521–8573.
- 7. Roudesly, F.; Oble, J.; Poli, G. Metal-catalyzed C-H activation/functionalization: The fundamentals. *J. Mol. Cat. A* **2017**, *426 (Part B)*, 275–296.
- 8. Hartwig, J. F.; Larsen, M. A. Undirected, Homogeneous C–H Bond Functionalization: Challenges and Opportunities. *ACS Cent. Sci.* **2016**, *2*, 281–292.
- 9. Vastine, B. A.; Hall, M. B. Carbon-Hydrogen Bond Activation: Two, Three, or More Mechanisms?. *J. Am. Chem. Soc.* **2007**, *129*, 12068–12069.
- 10. a) Lin, Z. Current understanding of the σ-bond metathesis reactions of LnMR+ R′–H→ LnMR′+ R–H. Coord. Chem. Rev. 2007, 251, 2280–2291. b) Waterman, R. σ-Bond Metathesis: A 30-Year Retrospective. Organometallics 2013, 32, 7249-7263.
- 11. Watson, P. L. Methane exchange reactions of lanthanide and early-transition-metal methyl complexes. *J. Am. Chem. Soc.* **1983**, *105*, 6491–6493.

- 12. Watson, P. L. Facile C–H activation by lutetium–methyl and lutetium–hydride complexes. *J. Chem. Soc., Chem. Commun.* **1983**, 276–277.
- 13. Watson, P. L. In *Selective Hydrocarbon Activation: Principles and Progress*; Davies, J. A., Watson, P. L., Greenberg, A., Liebman, J. F., Eds.; VCH: New York, 1990; p 79.
- 14. Watson, P. L.; Parshall, G. W. Organolanthanides in catalysis. Acc. Chem. Res. 1985, 18, 51–56.
- 15. Davies, J. A.; Watson, P. L.; Liebman, J. F.; Greenberg, A. *Selective Hydrocarbon Activation: Principles and Progress*; VCH Publishers: New York, 1990.
- 16. Perutz, R. N.; Sabo-Etienne, S. The σ-CAM mechanism: σ complexes as the basis of σ-bond metathesis at late-transition-metal centers. *Ang. Chem. Int. Ed.* **2007**, *46*, 2578–2592.
- 17. Jones, W. D. Isotope Effects in C–H Bond Activation Reactions by Transition Metals. *Acc. Chem. Res.* **2003**, *36*, 140–146.
- 18. Churchill, D. G.; Janak, K. E.; Wittenberg, J. S.; Parkin, G. Normal and Inverse Primary Kinetic Deuterium Isotope Effects for C–H Bond Reductive Elimination and Oxidative Addition Reactions of Molybdenocene and Tungstenocene Complexes: Evidence for Benzene σ-Complex Intermediates. *J. Am. Chem. Soc.* **2003**, *125*, 1403–1420.
- 19. Cowan, A. J.; George, M. W. Formation and Reactivity of Organometallic Alkane Complexes. *Coord. Chem. Rev.* **2008**, *252*, 2504–2511.
- 20. a) Asbury, J. B.; Hang, K.; Yeston, J. S.; Cordaro, J. G.; Bergman, R. G.; Lian, T. Direct Observation of a Picosecond Alkane C–H Bond Activation Reaction at Iridium. *J. Am. Chem. Soc.* **2000**, *122*, 12870–12871. b) Lugovskoy, A.; Paur-Afshari, R.; Schultz, R. H. Reaction of the Transient Species W(CO) 5(Cyclohexane) with Cyclo-C<sub>4</sub>H<sub>n</sub>O (*n* = 4, 6, 8) Studied by Time-Resolved Infrared Absorption Spectroscopy. *J. Phys. Chem. A* **2000**, *104*, 10587–10593.
- 21. Clot, E.; Eisenstein, O. Agostic interactions from a computational perspective: One name, many interpretations. From Structure and Bonding, Berlin, Germany, 2004, 113, Principles and Applications of Density Functional Theory in Inorganic Chemistry II, 1–36.

- 22. Balcells, D.; Clot, E.; Eisenstein, O. C–H Bond Activation in Transition Metal Species from a Computational Perspective. *Chem. Rev.* **2010**, *110*, 749–823.
- 23. Niu, S.; Hall, M. B. Theoretical Studies on Reactions of Transition-Metal Complexes. *Chem. Rev.* **2000**, *100*, 353–405.
- 24. a) Cobar, E. A.; Khaliullin, R. Z.; Bergman, R. G.; Head-Gordon, M. Theoretical study of the rhenium–alkane interaction in transition metal–alkane σ-complexes. *Proc. Natl. Acad. Sci. U.S.A.* **2007**, *104*, 6963–6968. b) Chan, B.; Ball, G. E. A Benchmark Ab Initio and DFT Study of the Structure and Binding of Methane in the σ–Alkane Complex CpRe(CO)<sub>2</sub>(CH<sub>4</sub>). *J. Chem. Theory Comput.* **2013**, *9*, 2199–2208.
- 25. a) Castro-Rodriguez, I.; Nakai, H.; Gantzel, P.; Zakharov, L. N.; Rheingold, A. L.; Meyer, K. Evidence for Alkane Coordination to an Electron-Rich Uranium Center. *J. Am. Chem. Soc.* **2003**, *125*, 15734–15735. b) Pike, S. D.; Thompson, A. L.; Algarra, A. G.; Apperley, D. C.; Macgregor, S. A.; Weller, A. S. Synthesis and Characterization of a Rhodium(I) σ-Alkane Complex in the Solid State. *Science* **2012**, *337*, 1648–1651. c) Chadwick, F. M.; Rees, N. H.; Weller, A. S.; Krämer, T.; Iannuzzi, M.; Macgregor, S. A. A Rhodium–Pentane Sigma-Alkane Complex: Characterization in the Solid State by Experimental and Computational Techniques. *Angew. Chem. Int. Ed.* **2016**, *55*, 3677–3681. d) McKay, A. I; Krämer, T.; Rees, N. H.; Thompson, A. L.; Christensen, K. E.; Macgregor, S. A.; Weller, A. S. Formation of a σ-alkane Complex and a Molecular Rearrangement in the Solid-State: [Rh(Cyp<sub>2</sub>PCH<sub>2</sub>CH<sub>2</sub>PCyp<sub>2</sub>)(η<sup>2</sup>:η<sup>2</sup>-C<sub>7</sub>H<sub>12</sub>)][BAr<sup>F</sup><sub>4</sub>]. *Organometallics* **2017**, *36*, 22–25. e) Martínez-Martínez, A. J.; Tegner, B. E.; McKay, A. I.; Bukvic, A. J.; Rees, N. H.; Tizzard, G. J.; Coles, S. J.; Warren, M. R.; Macgregor, S. A.; Weller, A. S. Modulation of σ-Alkane Interactions in [Rh(L<sub>2</sub>)(alkane)]<sup>+</sup> Solid-State Molecular Organometallic (SMOM) Systems by Variation of the Chelating Phosphine and Alkane: Access to η<sup>2</sup>, η<sup>2</sup>-σ-Alkane Rh(I), η<sup>1</sup>-σ-Alkane Rh(III) Complexes, and Alkane Encapsulation. *J. Am. Chem. Soc.* **2018**, *140*, 14958–14970.
- 26. Fukui, K. The Path of Chemical Reactions The IRC Approach. Acc. Chem. Res. 1981, 14, 363–368.

- 27. a) Carlsen, R.; Wohlgemuth, N.; Carlson, L.; Ess, D. H. Dynamical Mechanism May Avoid High-Oxidation State Ir(V)-H Intermediate and Coordination Complex in Alkane and Arene C-H Activation by Cationic Ir(III) Phosphine. *J. Am. Chem. Soc.* **2018**, *140*, 11039–11045. b) Carlsen, R.; Jenkins, J. R.; Ess, D. H. Molecular Dynamics Analysis of the Cationic Cp\*(PMe<sub>3</sub>)Ir(CH<sub>3</sub>) Methane C-H Activation Mechanism" *Faraday Discussions*, **2019**, *220*, 414–424.
- 28. Teynor, M. S.; Carlsen, R.; Ess, D. H. Relationship Between Energy Landscape Shape and Dynamics Trajectory Outcomes for Methane C-H Activation by Cationic Cp\*(PMe<sub>3</sub>)Ir/Rh/Co(CH<sub>3</sub>).

  Organometallics, 2020, 39, 1393–1403.
- 29. Smith, J. A.; Schouten, A.; Wilde, J. H.; Westendorff, K. S.; Dickie, D. A.; Ess, D. H.; Harmen, W. D. Experiments and Direct Dynamics Simulations Reveal a Network of Reaction Pathways for Tungsten  $\eta^2$ -Arene Aryl Hydride Equilibria. *J. Am. Chem. Soc.* **2020**, *142*, 16437–16454.
- 30. a) Sherer, E. C.; Cramer, C. J. Quantum Chemical Characterization of Methane Metathesis in  $L_2MCH_3$  (L = H, Cl, Cp, Cp\*; M = Sc, Y, Lu). *Organometallics* **2003**, *22*, 1682–1689. b) Lewin, J. L.; Woodrum, N. L.; Cramer, C. J. Density Functional Characterization of Methane Metathesis in *ansa*-[Bis( $\eta^5$ -2-indenyl)methane]ML Complexes [M = Sc, Y, Lu; L = CH<sub>3</sub>, CH<sub>2</sub>C(CH<sub>3</sub>)<sub>3</sub>]. *Organometallics* **2006**, *25*, 5906–5912.
- 31. a) Oxgaard, J.; Muller, R. P.; Goddard, W. A., III; Periana, R. A. Mechanism of homogeneous Ir (III) catalyzed regioselective arylation of olefins. *J. Am. Chem. Soc.* **2004**, *126*, 352–363. b) Oxgaard, J.; Periana, R. A.; Goddard, W. A., III Mechanistic analysis of hydroarylation catalysts. *J. Am. Chem. Soc.* 2004, 126, 11658–11665.
- 32. Webster, C. E.; Fan, Y.; Hall, M. B.; Kunz, D.; Hartwig, J. F. Experimental and Computational Evidence for a Boron-Assisted, *σ*-Bond Metathesis Pathway for Alkane Borylation *J. Am. Chem. Soc.* 2003, 125, 858–859.
- 33. Frisch, M. J.; Trucks, G. W.; Schlegel, H. B.; Scuseria, G. E.; Robb, M. A.; Cheeseman, J. R.; Scalmani, G.; Barone, V.; Mennucci, B.; Petersson, G. A.; Nakatsuji, H.; Caricato, M.; Li, X.; Hratchian,

H. P.; Izmaylov, A. F.; Bloino, J.; Zheng, G.; Sonnenberg, J. L.; Hada, M.; Ehara, M.; Toyota, K.;

Fukuda, R.; Hasegawa, J.; Ishida, M.; Nakajima, T.; Honda, Y.; Kitao, O.; Nakai, H.; Vreven, T.;

Montgomery, J. A., Jr.; Peralta, J. E.; Ogliaro, F.; Bearpark, M.; Heyd, J. J.; Brothers, E.; Kudin, K. N.;

Staroverov, V. N.; Kobayashi, R.; Normand, J.; Raghavachari, K.; Rendell, A.; Burant, J. C.; Iyengar, S.

S.; Tomasi, J.; Cossi, M.; Rega, N.; Millam, N. J.; Klene, M.; Knox, J. E.; Cross, J. B.; Bakken, V.;

Adamo, C.; Jaramillo, J.; Gomperts, R.; Stratmann, R. E.; Yazyev, O.; Austin, A. J.; Cammi, R.; Pomelli,

C.; Ochterski, J. W.; Martin, R. L.; Morokuma, K.; Zakrzewski, V. G.; Voth, G. A.; Salvador, P.;

Dannenberg, J. J.; Dapprich, S.; Daniels, A. D.; Farkas, Ö.; Foresman, J. B.; Ortiz, J. V.; Cioslowski, J.;

Fox, D. J. Gaussian 09, Revision B.01, Gaussian, Inc., Wallingford CT, 2010.

34. Zhao, Y.; Truhlar, D. G. The M06 Suite of Density Functionals for Main Group Thermochemistry,

Thermochemical Kinetics, Noncovalent Interactions, Excited States, and Transition Elements: Two New

Functionals and Systematic Testing of Four M06-Class Functionals and 12 Other Functionals. *Theor.* 

Chem. Acc. 2008, 120, 215–241.

35. a) Carpenter, Barry K. Energy Disposition in Reactive Intermediates. Chem. Rev. 2013, 113, 7265-

7286. b) Carpenter, Barry K. Dynamic behavior of organic reactive intermediates. Angew. Chem. Int. Ed.

Engl. 1999, 37, 3341–3350. c) Spezia, R.; Martínez-Nuñez, E.; Vazquez, S.; Hase, W. L. Perspective:

chemical dynamics simulations of non-statistical reaction dynamics. Phil. Trans. R. Soc. A 2017,

375:20170035. d) Lourderaj, U.; Park, K.; Hase, W. L. Classical trajectory simulations of post-transition

state dynamics. Int. Rev. Phys. Chem. 2009, 113, 2236–2253. e) Paranjothy, M.; Sun, R.; Zhuang, Y.;

Hase, W. L. Direct chemical dynamics simulations: coupling of classical and quasiclassical trajectories

with electronic structure theory. Wiley Interdisciplinary Reviews: Computational Molecular Science,

**2013**, *3*, 296–316.

36. a) Carpenter, B. K. Nonstatistical dynamics in thermal reactions of polyatomic molecules. Annual

Review of Physical Chemistry, 2005, 56, 57–89. b) Carpenter, Barry K. Potential energy surfaces and

reaction dynamics. Eds. Moss, R. A.; Platz, M. S.; Jones, M., Jr.; Reactive Intermediate Chemistry,

**2004**, 925–960. c) Xie, J.; Hase, W. L. Rethinking the S<sub>N</sub>2 reaction. *Science* **2016**, 352, 32–33. d)

Doubleday, C. Unusual Potential Energy Surfaces and Nonstatistical Dynamic Effects. in Applied Theoretical Organic Chemistry; Ed. Tantillo, D. J. e) Hare, S. R.; Tantillo, D. J. Post-transition state bifurcations gain momentum – current state of the field. Pure Appl. Chem. 2017, 89, 679–698. 37. a) Barros, N.; Eisenstein, O.; Maron, L. DFT studies of the methyl exchange reaction between Cp<sub>2</sub>M- $CH_3$  or  $Cp*_2M-CH_3$  ( $Cp=C_5H_5$ ,  $Cp*=C_5Me_5$ , M=Y, Sc, Ln) and  $CH_4$ . Does M ionic radius control the reaction?. Dalton Trans. 2006, 3052-3057. b) Maron, L.; Perrin, L.; Eisenstein, O. DFT study of CH<sub>4</sub> activation by  $d^0$  Cl<sub>2</sub>LnZ (Z = H, CH<sub>3</sub>) complexes. J. Chem. Soc., Dalton Trans., 2002, 534–539. 38. a) Wong-Foy, A. G.; Bhalla, G.; Liu, X. Y.; Periana, R. A. Alkane C- H Activation and Catalysis by an O-Donor Ligated Iridium Complex. J. Am. Chem. Soc. 2003, 125, 14292-14293. b) Periana, R. A.; Liu, X. Y.; Bhalla, G. Novel bis-acac-O, O-Ir (III) catalyst for anti-Markovnikov, hydroarylation of olefins operates by arene CH activation. Chem. Commun. 2002, 24, 3000–3001. c) Bhalla, G.; Oxgaard, J.; Goddard, W. A., III; Periana, R. A. Anti-markovnikov hydroarylation of unactivated olefins catalyzed by a bis-tropolonato iridium (III) organometallic complex. Organometallics 2005, 24, 3229–3232. d) Bhalla, G.; Liu, X. Y.; Oxgaard, J.; Goddard, W. A., III; Periana, R. A. CH Activation with an O-Donor Iridium-Methoxo Complex. J. Am. Chem. Soc. 2005, 127, 11372–11389. e) Bhalla, G.; Oxgaard, J.; Goddard, W. A. III; Periana R. A. Hydrovinylation of olefins catalyzed by an iridium complex via CH activation. Organometallics 2005, 24, 5499-5502. f) Oxgaard, Jonas; Tenn, William J., III; Nielsen, Robert J.; Periana, Roy A.; Goddard, William A., III Mechanistic analysis of iridium heteroatom C-H activation: Evidence for an internal electrophilic substitution mechanism. *Organometallics* **2007**, *26*, 1565–1567.

39. a) Waltz, K. M.; Hartwig, J. F. Selective functionalization of alkanes by transition-metal boryl complexes. *Science* **1997**, *277*, 211–213. b) Chen, H.; Schlecht, S.; Semple, T. C.; Hartwig, J. F. Thermal, catalytic, regiospecific functionalization of alkanes. *Science* **2000**, *287*, 1995–1997. c) Waltz, K. M.; Hartwig, J. F. Functionalization of alkanes by isolated transition metal boryl complexes. *J. Am. Chem. Soc.* **2000**, *122*, 11358–11369. d) Sawyer, K. R.; Cahoon, J. F.; Shanoski, J. E.; Glascoe, E. A.; Kling, M. F.; Schlegel, J. P.; Zoerb, M. C.; Hapke, M.; Hartwig, J. F.; Webster, C. E.; Harris, C. B. Time-resolved

IR Studies on the Mechanism for the Functionalization of Primary C-H Bonds by Photoactivated Cp\*W(CO)<sub>3</sub>(Bpin). *J. Am. Chem. Soc.* **2010**, *132*, 1848–1859.

- 40. a) Webster, Charles Edwin; Fan, Yubo; Hall, Michael B.; Kunz, Doris; Hartwig, John F. Experimental and computational evidence for a boron-assisted, σ-bond metathesis pathway for alkane borylation. *J. Am. Chem. Soc.* **2003**, *125*, 858–859.
- 41. Raynaud, C.; Daudey, J.-P.; Jolibois F.; Maron, L. Ab Initio Dynamic Study of the Reaction of Cl<sub>2</sub>LaR (R = H, CH<sub>3</sub>) with H<sub>2</sub>. *J. Phys. Chem. A*, **2006**, *110*, 101–105.
- 42. a) Neese, F. The ORCA Program System. *Comput. Mol. Sci.* **2012**, *2*, 73–78. b) Lu, Q.; Neese, F.; Bistoni, G. London dispersion effects in the coordination and activation of alkanes in σ-complexes: a local energy decomposition study. *Phys. Chem. Chem. Phys.* **2019**, *21*, 11569–11577.

# TOC graphic

